1, 2 and 3 in the sequences of cadmium iodide polytypic structures is understandable on the basis of formation of polytypes in terms of the creation of possible stacking faults in the basic structure. The occurrence of higher Zhdanov numbers is forbidden because these lead to sequences which involve adjacent layers in similar orientations; the higher Zhdanov numbers are, therefore, not feasible. Although the present investigation is confined to the understanding of the occurrence of certain specific Zhdanov numbers in cadmium iodide polytypic structures, similar analysis can be developed for the preponderance of certain specific Zhdanov numbers in polytypic crystals which have their basic structures resembling that of cadmium iodide, such as lead iodide, cadmium bromide *etc.*

The authors are thankful to Dr G. S. Verma, Head of the Department of Physics, Banaras Hindu University, Varanasi-5 and to Dr A. R. Verma, Director, National Physical Laboratory, New Delhi for their interest in the present work. The present work has been carried out with financial support from the Council of Scientific and Industrial Research, New Delhi.

References

CHADHA, G. K. & TRIGUNAYAT, G. C. (1967). *Acta Cryst.* **22**, 573.
JAGODZINSKI, H. (1954). *Acta Cryst.* **7**, 300.
PRASAD, R. (1971). Ph.D. Thesis, Banaras Hindu University.
PRASAD, R. & SRIVASTAVA, O. N. (1970*a*). *Z. Kristallogr.* **131**, 376.
PRASAD, R. & SRIVASTAVA, O. N. (1970*b*). *J. Phys. D: Appl. Phys.* **3**, 91.
PRASAD, R. & SRIVASTAVA, O. N. (1971*a*). *Acta Cryst.* A**27**, 259.
PRASAD, R. & SRIVASTAVA, O. N. (1971*b*). *J. Appl. Cryst.* **4**, 516.
PRASAD, R. & SRIVASTAVA, O. N. (1971*c*). *Z. Kristallogr.* In the press.
SIEMS, R., DELVIGNETTE, P. & AMELINCKX, S. (1964). *Phil. Mag.* **9**, 121.
SRIVASTAVA, O. N. & VERMA, A. R. (1964). *Acta Cryst.* **17**, 260.
SRIVASTAVA, O. N. & VERMA, A. R. (1965). *Acta Cryst.* **19**, 56.
TRIGUNAYAT, G. C. & CHADHA, G. K. (1971). *Phys. Stat. Sol.* (*a*), *4*, 9.
TRIGUNAYAT, G. C. (1971). *Phys. Stat. Sol.* (*b*), **4**, 281.
VERMA, A. R. & KRISHNA, P. (1966). *Polymorphism and Polytypism in Crystals.* New York: Wiley.

Acta Cryst. (1972). A**28**, 497

Twinning in 5,5′-Biisoxasole

BY M. CANNAS, G. CARTA AND G. MARONGIU
Istituto Chimico dell'Università, 09100 *Cagliari, Italy*

(*Received* 22 *March* 1972)

Weissenberg photographs from triclinic 5,5′-biisoxasole are explained in terms of three twinning laws defined as [001], (100) and (010). A structural interpretation of the twins is proposed using the results of the structure determination.

In a previous paper (Cannas & Marongiu, 1968) the crystal structure of 5,5-biisoxasole, determined by three-dimenisional X-ray diffraction data, was reported.

Crystal data

5,5′-biisoxasole $C_6H_4N_2O_2$, M.W. 136·11, m.p. 161 °C, $a=10{\cdot}47\pm0{\cdot}02$, $b=9{\cdot}01\pm0{\cdot}02$, $c=3{\cdot}78\pm0{\cdot}01$ Å,

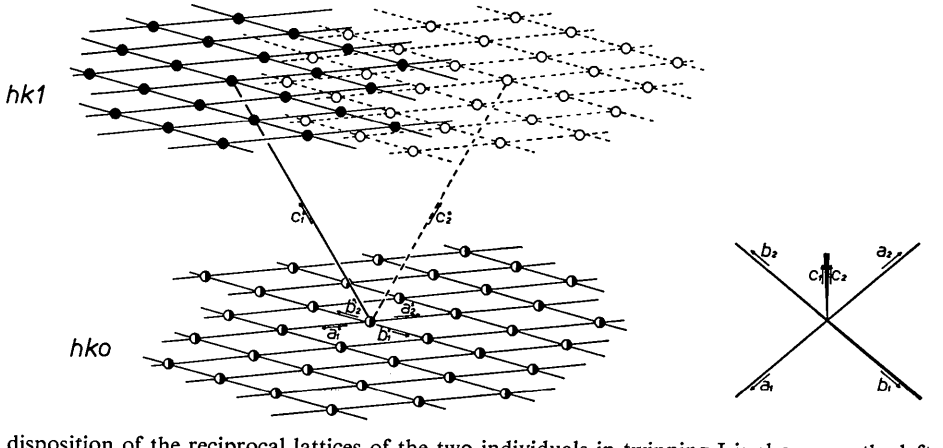

Fig. 1. The relative disposition of the reciprocal lattices of the two individuals in twinning I is shown on the left. On the right is given the relative orientation of the direct axes.

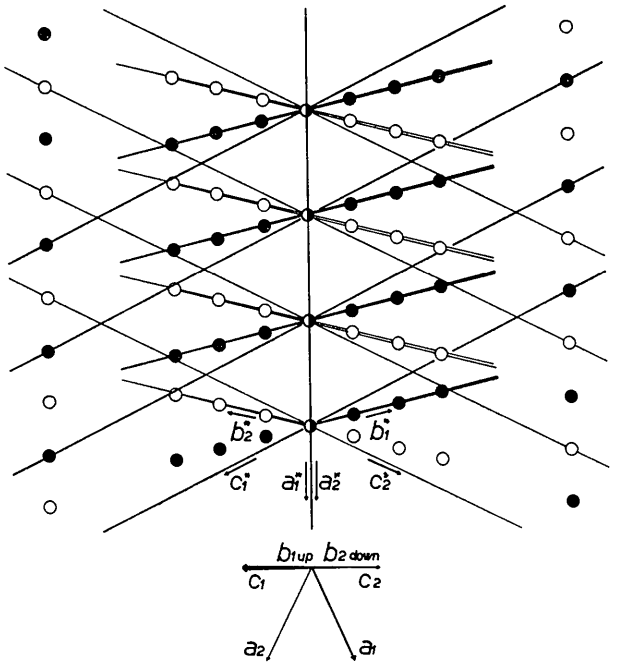

Fig. 2. The relative disposition of the reciprocal lattices of the two individuals in twinning II (top) and the relative orientation of the direct axes (bottom).

$\alpha = 75°58' \pm 15'$, $\beta = 115°46' \pm 20'$, $\gamma = 90°51' \pm 20'$,
$V = 309{\cdot}8$ Å^3, $Z = 2$,
$D_x = 1{\cdot}46$ g.cm^{-3}, $D_m = 1{\cdot}43$ g.cm^{-3}.
Space group $P\bar{1}$ (from structure analysis).

In the course of preliminary data collection for the X-ray analysis, some difficulties arose in the choice of a suitable sample, since all the crystals appear to be twinned; in an attempt to select a single crystal out of the batch obtained by slow evaporation of an ethyl alcohol solution, three different types of twinning were detected.

An analysis of the geometrical and structural relationships in the three types of twinning (herein referred as twinning I, II, III) has been now completed and the results are reported in this paper.

Geometrical relationships

Twinning I

The oscillation and equatorial Weissenberg photographs taken around the *c* axis agree with a triclinic lattice symmetry, while the upper level photographs show C_2 pseudo-symmetry. This fact is interpreted, on the basis of the reciprocal parameters derived from the equatorial layer, by assuming that, due to twinning, there are two non-coincident reciprocal lattices. From the analysis of the photographs it emerged that the a^* and b^* axes of the two individuals in twin orientation coincide but point in opposite directions (which explains the unique $hk0$ net) while the c^* axes diverge; as a consequence, upper levels of the reciprocal lattices of the two individuals are displaced one with respect to the other; coincidence of the lattices will be obtained by a 180° rotation about [001], which is the twin axis.

A diagrammatical view of the lattices and the orientation of direct and reciprocal axes of the two individuals are given in Fig. 1.

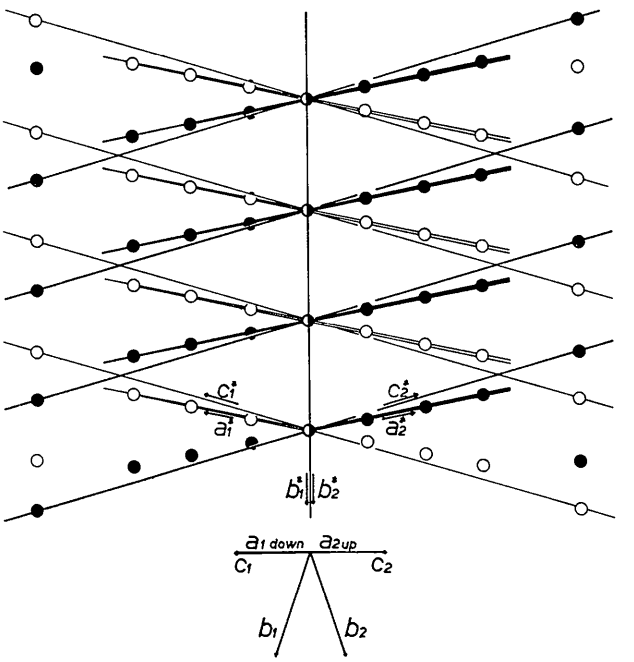

Fig. 3. The relative disposition of the reciprocal lattices of the two individuals in twinning III (top) and the relative orientation of the direct axes (bottom).

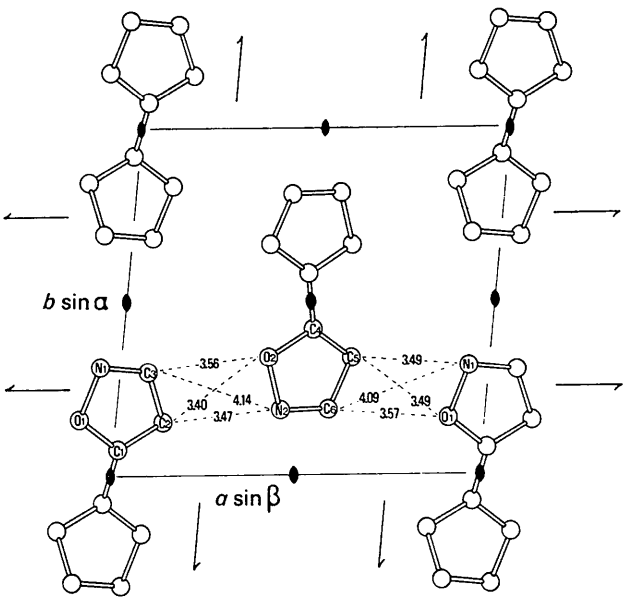

Fig. 4. Projection of the crystal structure along c. Pseudo-symmetry elements and closest intermolecular contacts are given.

Twinning II

Both *hk*0 and *h*0*l* Weissenberg photographs show C_{2l} symmetry: the *h*00 row appears once in both of them and acts as a symmetry line; the 0*k*0 and 00*l* rows on the other hand are seen twice and a symmetry line, 90° away from the a^* axis, appears along the bisector of the angle between the b_1^* and b_2^* directions in the *hk*0 net, and between the c_1^* and c_2^* directions in the *h*0*l* net. As shown in Fig. 2, it results that the two individuals share the a^* axis, while the b^* and c^*

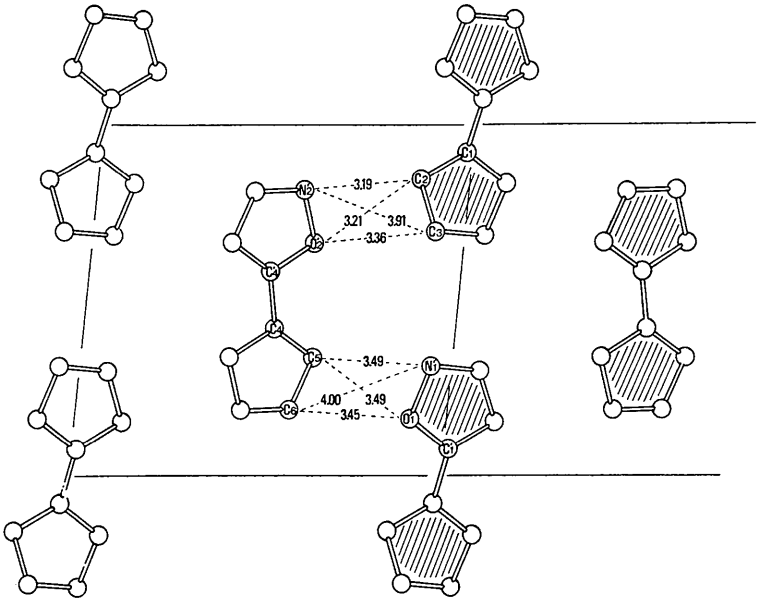

Fig. 5. Projection of the structure of the two individuals at the boundary layer for twinning I. Quoted intermolecular contacts refer to the case where pseudo-symmetry (twofold axis coincident with c) is applied to the molecule in 000. Intermolecular contacts which result by applying pseudo-symmetry to the molecule in $\frac{1}{2}\frac{1}{2}0$ are: C(2*A*)–N′(2*B*)=3·41 Å; C(3*A*)–O′(2*B*)=3·40 Å; C(2*A*)–O′(2*B*)=3·29 Å; C(3*A*)–N′(2*B*)=4·08 Å; N′(1*A*)–C(5*B*)=3·26 Å; O′(1*A*)–C(6*B*)=3·32 Å; N′(1*A*)–C(6*B*)=3·99 Å; O′(1*A*)–C(5*B*)=3·13 Å. *A* refers to atoms in the structure, *B* to those in the twin.

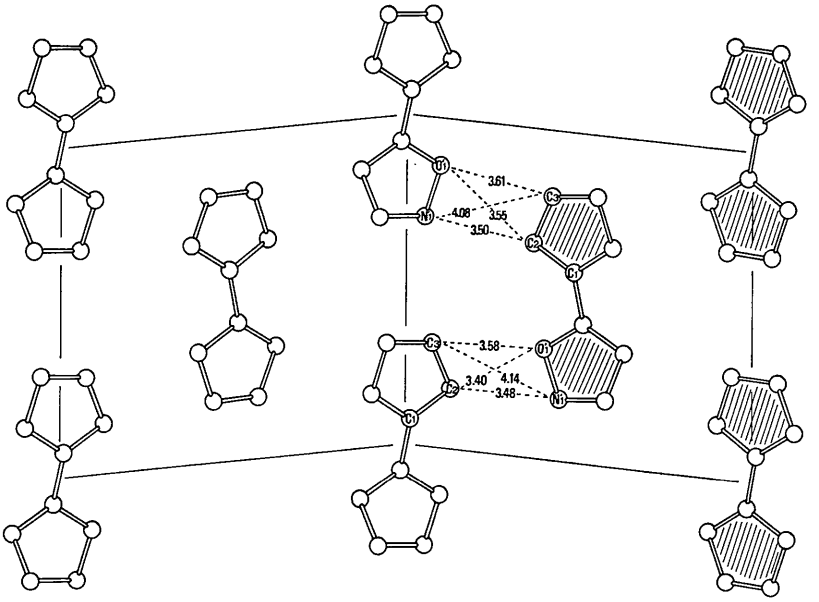

Fig. 6. Projection of the structure of the two individuals at the boundary layer for twinning II. Quoted intermolecular contacts refer to the case where pseudo-symmetry (two-fold screw-axis parallel to **b** through $x=\frac{1}{4}$, $z=0$) is applied to the molecule in 000. Intermolecular contacts which result by applying pseudo-symmetry to the molecule in $\frac{1}{2}\frac{1}{2}0$ are: N(2*A*)–C′(5*B*)=3·27 Å; O(2*A*)–C′(6*B*)=3·43 Å; O(2*A*)–C′(5*B*)=3·24 Å; N(2*A*)–C′(6*B*)=4·01 Å; C′(5*A*)–N(2*B*)=3·47 Å; C′(6*A*)–O(2*B*)=3·55 Å; C′(5*A*)–O(2*B*)=3·50 Å; C′(6*A*)–N(2*B*)=4·08 Å. *A* refers to atoms in the structure, *B* to those in the twin.

axes diverge; those appearing in the photographs across the symmetry line have opposite directions. Coincidence of the lattices of the two individuals will be obtained by a 180° rotation about **a***, the normal to (100), which is therefore the twin plane.

Twinning III

The *hk*0 Weissenberg photograph, the only one taken for this type of twinning, shows, as in twinning II, C_{2l} symmetry: symmetry lines are the b^* axis, common to both individuals, and the line between $\mathbf{a}_1^*$ and $\mathbf{a}_2^*$, which make an angle of $\simeq 12°$. The orientation of the direct and reciprocal axes of the two individuals is similar to that of twinning II and is shown in Fig. 3. Coincidence of the lattices of the two individuals is obtained by a 180° rotation about **b***, the normal to (010), which is the twin plane.

Structural relationships

The projection of the crystal structure along the *c* axis is shown in Fig. 4. The molecule is centrosymmetric, and the asymmetric unit is half of one molecule in 000 and half of the one in $\frac{1}{2}\frac{1}{2}0$ (Wyckoff notations *a* and *e* respectively). In Fig. 4 are also shown the following three pseudo-symmetry elements in the structure:

(*a*) a pseudo-twofold axis coincident with **c**,
(*b*) a pseudo-twofold screw-axis parallel to **b** through $x=\frac{1}{4}$, $z=0$,
(*c*) a pseudo-twofold screw-axis parallel to **a** through $y=\frac{1}{4}$, $z=0$.

Application of the symmetry operations, corresponding to the above-mentioned pseudo-elements, gives boundary structures which are consistent with the three experimental twin laws. According to whether the symmetry operation is applied to one or the other molecule in the unit cell, two boundary layers result for each type of twinning; in the following figures we report for simplicity's sake only the case where symmetry is applied to the molecule in 000.

Twinning I

The orientation of the structure of the second individual with respect to the first is obtained by a 180° rotation of the crystal structure about **c**, the twin axis. As a result of this operation atoms in individual *B* are related to those in individual *A* by the following relations:

$$x_A=x_B;\quad y_A=y_B;\quad z_A=-z_B\,.$$

Molecular contacts across the twin boundary calculated according to the above relations are shown in Fig. 5.

Twinning II

In Fig. 6 are shown the structural conditions at the boundary layer; it can easily be seen that the (100) plane acts in agreement with the twin law, as a symmetry plane for the lattice, but not for the structure. The molecules of the twin are in fact related to those of the crystal by a twofold screw axis parallel to **b** through $\frac{1}{4}00$.

Atomic coordinates in individual *B* are related to those in individual *A* by the following relations:

$$x_B=-\tfrac{1}{2}-x_A;\quad y_B=\tfrac{1}{2}+y_A;\quad z_B=-z_A\,.$$

Molecular contacts at the boundary layer are shown in Fig. 6.

Twinning III

In this type of twinning the symmetry operation which relates molecules at the boundary layer is the two-fold screw-axis parallel to *a* through $0\frac{1}{4}0$. The structural conditions at the boundary layer are shown in Fig. 7; in the same figure are quoted the closest intermolecular contacts between atoms in the two indivials, for which the following coordinate relationships hold:

$$x_B=\tfrac{1}{2}+x_A;\quad y_B=\tfrac{1}{2}-y_A;\quad z_B=-z_A\,.$$

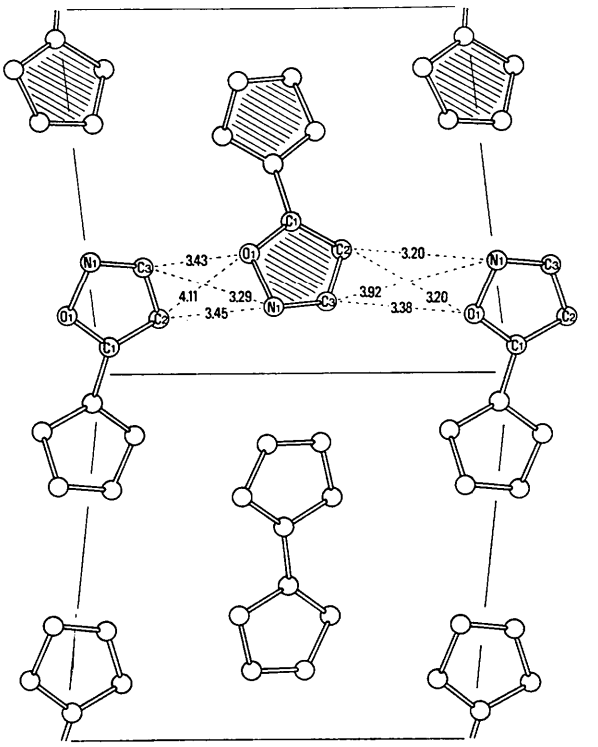

Fig. 7. Projection of the structure of the two individuals at the boundary layer for twinning III. Quoted intermolecular contacts refer to the case where pseudo-symmetry (two-fold screw-axis parallel to **a** through $y=\frac{1}{4}$, $z=0$) is applied to the molecule in 000. Intermolecular contacts which result by applying pseudo-symmetry to the molecule in $\frac{1}{2}\frac{1}{2}0$ are: C(5*A*)–N(2*B*) = 3·42 Å; C(6*A*)–O(2*B*) = 3·39 Å; C(5*A*)–O(2*B*) = 3·32 Å; C(6*A*)–N(2*B*) = 4·03 Å; N(2*A*)–C(5*B*) = 3·27 Å; O(2*A*)–C(6*B*) = 3·43 Å; N(2*A*)–C(6*B*) = 4·01 Å; O(2*A*)–C(5*B*) = 3·23 Å. *A* refers to atoms in the structure, *B* to those in the twin.

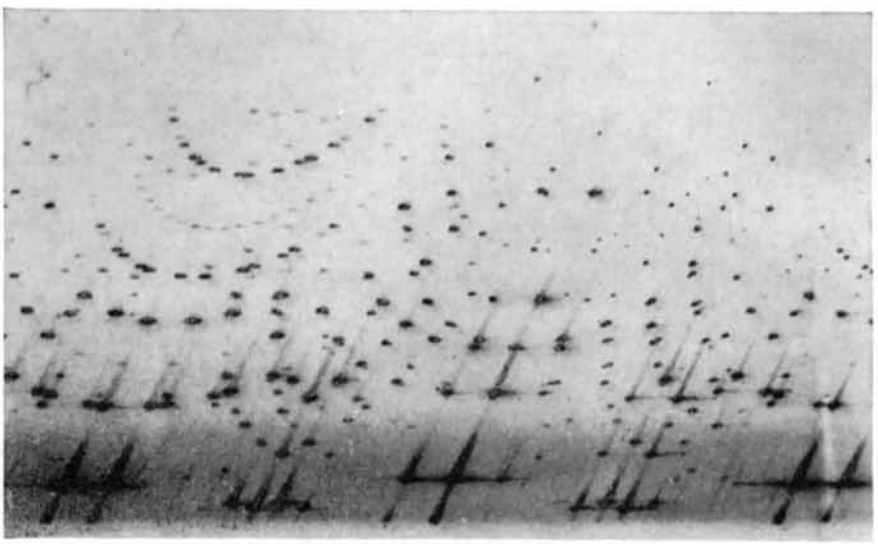

Fig. 8. *hk*0 Photograph of a multi-twinned crystal.

[*To face p.* 501

General remarks

Statistical distribution of the twins, carried out on about thirty crystals from the same batch, has shown that twinning I is by far the most frequent of the three types; as is seen from X-ray intensities, crystals twinned according to this law have approximately equal volumes of the two components, thus suggesting the occurrence of multiple twinning; they moreover do not, in general, show either of the other two types of twinning: in the few cases where an individual twinned according to II or III is present, its volume is remarkably small. Twinning III is the least frequent and it generally occurs in those crystals which are also twinned according to II. A typical example of twinning II and III in the same crystal, where the volumes of the individuals happen to be approximately equal, is shown in Fig. 8.

At the boundary layers the molecules are packed in such a way that CH bonds are directed through oxygen and nitrogen atoms of adjacent molecules; this feature is present in the crystal structures of this compound and of the other investigated biisoxasole isomers (Cannas & Marongiu, 1967; Biagini, Cannas & Marongiu, 1969); from the values of intermolecular contacts at the boundary layers, which are very close to those found in the mentioned crystal structures, it could be inferred that the energy at the twin boundaries should not be much different from that of the regular structure.

This work was supported by the Italian Consiglio Nazionale delle Ricerche.

References

BIAGINI, S., CANNAS, M. & MARONGIU, G. (1969). *Acta Cryst.* B25, 730.

CANNAS, M. & MARONGIU, G. (1967). *Z. Kristallogr.* **124**, 143.

CANNAS, M. & MARONGIU, G. (1968). *Z. Kristallogr.* **127**, 388.

Acta Cryst. (1972). A28, 501

Polarization Phenomena in X-ray Diffraction

BY P. SKALICKY* AND C. MALGRANGE

Laboratoire Minéralogie Cristallographie, Université Paris VI, 9 *quai St Bernard, Tour* 16, *Paris Vème, France*

(*Received* 11 *November* 1971 *and in revised form* 16 *June* 1972)

Because of the dielectric properties of most crystals in the X-ray frequency region, polarization phenomena such as birefringence and optical activity are not found with X-rays in simple transmission. It can however be deduced from the dynamical theory that such effects occur in crystal diffraction. An experiment is described which proves that under certain conditions all four branches of the dispersion surface can be excited by linearly polarized incident waves. This means that elliptically polarized X-rays can also be produced by crystal diffraction. Therefore in principle all polarization experiments that can be performed with visible light are also possible with X-rays.

1. Introduction

Polarization phenomena which are observed with visible light (such as birefringence and optical activity) are generally not found for X-rays. This is because of the dielectric properties of most materials in the X-ray frequency region. Little attention has however been paid to the fact that polarization phenomena similar to those observed with visible light occur in crystal diffraction. This can be demonstrated by considering the influence of polarization on dynamical diffraction effects. One such effect which is sensitive to the state of polarization of crystal waves is the occurrence of Pendellösung fringes in the diffraction patterns from wedge-shaped crystals, which was first observed by Kato & Lang (1959). An explanation of Pendellösung fringes in terms of spherical wave theory was given by Kato (1961). Furthermore the effect of X-ray polarization on these fringes was investigated by two groups of authors: by Hattori, Kuriyama & Kato (1965) and by Hart & Lang (1965). They have shown that an unpolarized incident wave causes a fading of the fringes which can be explained as a superposition of two sets of fringes corresponding to waves with their polarization vectors parallel and perpendicular to the plane of incidence respectively. Besides that, Hart & Lang showed that there is only one set of fringes (and naturally no fading) when the incident wave is polarized perpendicular to the plane of incidence.

Still one important case remains to be investigated. This is the case of a linearly polarized incident beam with an electric vector making an angle different from 0 or 90° with the plane of incidence. From the theoretical results of Molière (1939) one can deduce that the diffraction of such a wave will give rise to elliptically

* Present address: Institute of Applied Physics, Technische Hochschule, Vienna, Austria.